Chemical Engineering Science 64 (2009) 4262 – 4277

Contents lists available at ScienceDirect

Chemical Engineering Science

journal homepage: www.elsevier.com/locate/ces

A control oriented study on the numerical solution of the population balance equation for crystallization processes

Ali Mesbah[a,b,*], Herman J.M. Kramer[b], Adrie E.M. Huesman[a], Paul M.J. Van den Hof[a]

[a]Delft Center for Systems and Control, Delft University of Technology, Mekelweg 2, 2628 CD Delft, The Netherlands
[b]Process and Energy Laboratory, Delft University of Technology, Leeghwaterstraat 44, 2628 CA Delft, The Netherlands

ARTICLE INFO

Article history:
Received 5 February 2009
Received in revised form 15 June 2009
Accepted 19 June 2009
Available online 25 June 2009

Keywords:
Dynamic simulation
Crystallization
Population balance
Nucleation
Growth
On-line control

ABSTRACT

The population balance equation provides a well established mathematical framework for dynamic modeling of numerous particulate processes. Numerical solution of the population balance equation is often complicated due to the occurrence of steep moving fronts and/or sharp discontinuities. This study aims to give a comprehensive analysis of the most widely used population balance solution methods, namely the method of characteristics, the finite volume methods and the finite element methods, in terms of the performance requirements essential for on-line control applications. The numerical techniques are used to solve the dynamic population balance equation of various test problems as well as industrial crystallization processes undergoing simultaneous nucleation and growth. The time-varying supersaturation profiles in the latter real-life case studies provide more realistic scenarios to identify the advantages and pitfalls of a particular numerical technique.

The simulation results demonstrate that the method of characteristics gives the most accurate numerical predictions, whereas high computational burden limits its use for complex real crystallization processes. It is shown that the high order finite volume methods in combination with flux limiting functions are well capable of capturing sharp discontinuities and steep moving fronts at a reasonable computational cost, which facilitates their use for on-line control applications. The finite element methods, namely the orthogonal collocation and the Galerkin's techniques, on the other hand may severely suffer from numerical problems. This shortcoming, in addition to their complex implementation and low computational efficiency, makes the finite element methods less appealing for the intended application.

1. Introduction

Substantial amounts of material in pharmaceutical, chemical and food industries are produced in crystalline form. Crystallization is a key separation unit in these industries, with a profound impact on plant operation and economics. An important quality aspect of the crystalline product is the crystal size distribution. Producing crystals of predefined size distribution often poses a major challenge in industrial crystallization processes. The mechanisms that dictate the evolution of the crystal size distribution are formation of new crystals as well as growth breakage and agglomeration of existing crystals. These phenomena are related to the kinetics, thermodynamics and other micro-scale phenomena including mass and heat transfer between the different phases present in the system. They are typically highly nonlinear functions of process variables, namely concentration and temperature.

In the recent years, dynamic modeling of crystallization processes has received considerable attention due to its importance in process synthesis, design and control. The population balance is a well established mathematical framework for dynamic modeling of numerous particulate systems such as polymerization, precipitation, etc.; see Ramkrishna (2000). This theory, which was originally put forward by Hulbert and Katz (1964) as an approach to model crystallization systems, describes the evolution of crystal identities during the crystallization process. The population balance modeling framework in fact provides a deterministic description of the dynamic distribution of the crystal size by forming a balance to calculate the number of crystals in the crystallizer. The solution of such a balance is the distribution of the number of crystals across the temporal and spatial domains, where the spatial domain may include both internal and external coordinates. The external coordinates typically consist of the ordinary rectangular coordinate system specifying the location of the crystals in the crystallizer, whereas the internal coordinates represent the characteristic size of the crystals.

* Corresponding author at: Delft Center for Systems and Control, Delft University of Technology, Mekelweg 2, 2628 CD Delft, The Netherlands.
E-mail address: ali.mesbah@tudelft.nl (A. Mesbah).

0009-2509/$ - see front matter © 2009 Elsevier Ltd. All rights reserved.
doi:10.1016/j.ces.2009.06.060

In industrial applications, the crystallizer is often assumed to be well mixed. As a result, the population balance equation (PBE) is only expressed in terms of the internal coordinates. Under this condition, the one-dimensional PBE for a crystallization process undergoing simultaneous nucleation and growth can be written as

$$\frac{\partial n(L,t)}{\partial t} + \frac{\partial (G(L,t)n(L,t))}{\partial L} = B(L,t) + Q(L,t,n), \tag{1}$$

where $n(L,t)$ is the number density function, t denotes the time, L is the internal coordinate, i.e. characteristic length, $G(L,t)$ is the growth/dissolution rate, $B(L,t)$ is the nucleation rate and $Q(L,t,n)$ signifies crystals entering or leaving the crystallizer.

A common practice in industrial batch crystallization is to run seeded batches in order to avoid undesirable phenomena such as primary nucleation and agglomeration that often adversely influence the crystal size distribution. Furthermore, the secondary nucleation most likely only produces infinitesimally small crystals in seeded batch runs. For these processes, Eq. (1) can be simplified to the following partial differential equation:

$$\frac{\partial n(L,t)}{\partial t} + \frac{\partial (G(L,t)n(L,t))}{\partial L} = 0 \tag{2}$$

with the left boundary condition

$$n(L_0,t) = \frac{B_0(t)}{G|_{L_0}}, \tag{3}$$

where B_0 denotes the total nucleation rate. It is worth noting that Eq. (2) is a hyperbolic partial differential equation due to the convection term $\partial(G(L,t)n(L,t))/\partial L$.

One of the oldest and most widely used methods to solve the PBE is the method of moments (Hulbert and Katz, 1964; Randolph and Larson, 1988). In this technique, the PBE is transformed into a set of ordinary differential equations that gives the exact solution for moments of the distribution, but cannot retrieve the full distribution. Analytical solution of the PBE, however, encounters a practical barrier in the majority of industrial crystallization systems as their PBE formulation for any combination of crystallization mechanisms cannot be reduced to the moment equations. Lack of analytical solutions for these systems necessitates the recourse to numerical solution techniques.

Accurate numerical solution of the PBE, on the other hand, is often challenging due to a variety of reasons. Common problems associated with the numerical solution of Eq. (2) for seeded batch systems include numerical diffusion and instability. The former problem usually stems from incompatibility between the initial condition and the boundary condition. The number density distribution of the seeds is unlikely to be the same as that generated due to the nucleation. In case that their values match, the first derivative of the distribution may not be identical. This can lead to sharp discontinuities that are rapidly broadened by numerical diffusion (Mahoney and Ramkrishna, 2002). The occurrence of steep moving fronts, which is a prime source of numerical instability, is the other frequently encountered difficulty in solving Eq. (2); this problem arises from the convective nature of growth dominated processes.

The foregoing complexities related to the numerical solution of the PBE have awakened the attention in many researchers to develop specialized algorithms. Several numerical solution techniques for the PBE are therefore proposed in the literature that can be roughly classified into four broad categories, namely finite difference methods, discretization techniques, the method of weighted residuals and Monte Carlo methods.

Finite difference methods are the frequently used general approach for solving partial differential equations. These schemes, however, may not be the best choice for numerical solution of the PBE, given the hyperbolic nature of the differential equation. Finite difference methods often lead to broadening of the sharp discontinuities due to numerical diffusion (Mahoney and Ramkrishna, 2002). Furthermore, they guarantee number and mass conservation of the population only in the limit of infinite resolution (Patankar, 1980). These drawbacks, along with the inherent complexity of choosing stable integration schemes, may make the use of the finite difference methods less appealing. Performance analysis of a number of finite difference methods for a system undergoing nucleation and growth can be found in Muhr et al. (1996) and Wojcik and Jones (1998). Recently, Bennett and Rohani (2001) have applied a combined Lax-Wendroff/Crank-Nicholson method to solve the PBE; the method exhibits rather promising results, which are free from numerical instabilities.

Discretization techniques comprise a wide variety of numerical methods including discretized population balances and finite volume methods. In the discretized population balance equations (Baterham and Hall, 1981; Hounslow et al., 1988), the inde pendent variable, namely the spatial domain, is divided into a finite number of intervals. The mean-value theorem is then employed to convert the continuous PBE into a series of discrete equations that are expressed in terms of either the number of crystals, called the M-I approach, or the average population density in each interval, called the M-II approach. Subsequently, the resulting set of stiff nonlinear differential algebraic equations is integrated numerically. The discretized population balance equations have been extensively exploited in the literature to simulate and optimize various crystallization applications (Marchal et al., 1990; David et al., 1991; Litster et al., 1995; Matthews and Rawlings, 1998; David et al., 2003). This technique typically allows accurate determination of the desired characteristics of the distribution, though construction of the entire distribution may be subject to severe errors. The discretized population formulation does have a major drawback. In many cases it exhibits either oscillatory behavior, resulting in negative number densities, or suffers from numerical diffusion at the discontinuous moving fronts. The latter problem emerges when the discrete version of a partial differential equation corresponds to a different original equation, one with an added diffusion term (Lapidus and Pinder, 1982). As will be explained later, Kumar and Ramkrishna (1997) proposed a modified formulation of the discretized population balance equations, referred to as the method of characteristics (MOC), to alleviate the foregoing shortcoming of this technique. The method of characteristics that is well capable of capturing the sharp fronts using moving size intervals has received a great deal of attention in the crystallization modeling and optimization applications (Lim et al., 2002; Hu et al., 2005a; Qamar and Warnecke, 2007). Paengjuntuek et al. (2008) used the MOC formulation proposed by Hu et al. (2005b) for batch to batch optimization and nonlinear control of seeded crystallization processes. Recently, Nagy (2009) used a novel efficient approach that combines the method of characteristics and the quadrature method of moments to solve the PBE aiming at model-based supersaturation control of a seeded batch crystallization process in a robust optimization framework.

The discretization techniques also encompass another category of numerical schemes known as the finite volume methods (FVMs) that were originally applied in the areas of fluid dynamics (Versteeg and Malalasekera, 1995). Owing to their formulation which enables one to cope with the convective nature of hyperbolic partial differential equations, they have become increasingly popular for numerical solution of the population balance equation in crystallization processes (Gerstlauer et al., 2001; Ma et al., 2002; Gunawan et al., 2004; Qamar et al., 2006). As will be shown, the high order finite volume methods in combination with flux limiting functions, also known as the high resolution schemes, typically lead to high order accuracy on a coarse grid mesh by resolving sharp discontinuities and suppressing numerical oscillations.

Another class of methods often used to solve the population balance equation is the method of weighted residuals, which is a general technique for the solution of partial differential equations. The methods associated with this technique retrieve the full distribution by approximating the solution with a series of basis functions, whose coefficients are specified such that their sum satisfies the PBE. The formulation of these methods is largely determined by the choice of the basis function, namely global and local functions. The use of the global basis functions is limited to problems in which the shape of the resulting distribution is known a priori as these functions cannot accommodate sharp changes and discontinuities of an arbitrarily-shaped distribution (Rigopoulos and Jones, 2003). On the contrary, to restore the generality and flexibility of the numerical method by capturing highly irregular distributions, local basis functions that lead to the so-called finite element formulation can be utilized. There is a vast number of studies reported in the literature in which the finite element methods are used to solve the PBE in crystallization systems (Gelbard and Seinfeld, 1978; Nicmanis and Hounslow, 1998; Mahoney and Ramkrishna, 2002; Alexopoulos et al., 2004). The major superiority of these methods over the finite difference methods and the discretization techniques is retrieval of the entire distribution as well as their flexibility in coping with any possible formulation of the PBE (Rigopoulos and Jones, 2003). Nonetheless, the finite element methods are more difficult to implement, computationally involved and, more importantly, incapable of dealing with discontinuous distributions as well as steep moving fronts. This technique will be further discussed in this paper.

Contrary to the above discussed deterministic methods, the PBE can also be solved by using the probabilistic Monte Carlo method (Maisels et al., 1999; Song and Qiu, 1999; Meimaroglou et al., 2006). In this approach, the histories of individual crystals, each exhibiting random behavior in accordance with a probabilistic function, are tracked by means of the Markov conditional probability. The Monte Carlo methods are more suitable for multivariate problems, where the foregoing numerical approaches usually become less efficient (Rigopoulos and Jones, 2003).

In general, demands on the solution method of the PBE differ with the nature of the application and the crystallization system under consideration. Recent developments in optimization tools as well as on-line measurement techniques, e.g. particle size distribution and concentration measurement technologies, have led to new opportunities for closed loop model-based observation and control of crystallization processes (Crowley et al., 2000; Shi et al., 2006; Mesbah et al., 2008). This work therefore primarily aims at scrutinizing PBE solution methods that are expected to best suit on-line process control applications. It is self-evident that in these applications computational burden of the numerical technique is of paramount importance as control actions need to be computed in a real-time setting. Closed loop implementation of a model-based control strategy however permits tolerance of reduced accuracy through the estimation of system states using the available on-line measurements.

This paper is intended to give a comprehensive analysis of the most widely used PBE solution methods in terms of the performance requirements essential for real-time control of crystallization processes. Several extensive reviews on the solution of the PBE can be found in the literature, where different numerical techniques such as the method of moments, the discretized population balance equations and the method of weighted residuals have been reviewed (Ramkrishna, 1985; Costa et al., 2007). However, the distinct contribution of this work is the diversity and comprehensiveness of the case studies, by which the various PBE solution methods are examined comparatively. The numerical techniques are not only assessed based on the test problems commonly used in the literature, but also applied to industrial case studies with varying supersaturation profiles to investigate their applicability to dynamic simulation of real crystallization processes. The latter case studies provide more realistic scenarios to better identify the advantages and pitfalls of a particular numerical technique.

In this work, the method of characteristics, the finite volume methods and the finite element methods have been comparatively studied. The method of characteristics and the finite volume methods are known to be capable of dealing with the numerical diffusion as well as the instability problems on a coarse grid mesh that make them particularly amenable to on-line control applications due to their improved computational efficiency. The finite element methods, on the other hand, allow exact prediction of the entire distribution that is essential when control of the full crystal size distribution is sought. The numerical techniques are examined in terms of their numerical accuracy, computational efficiency and implementation-related issues for crystallization processes undergoing simultaneous nucleation and growth. Depending on the choice of the dynamic optimization strategy, namely sequential, simultaneous and multiple-shooting, used for the on-line control application, the computational efficiency of dynamic simulations may serve as an indication for the computational burden required for dynamic optimization of the crystallization process under study.

In what follows, formulations of the method of characteristics, the finite volume methods and the finite element methods are discussed in Sections 2–4, respectively. This is followed by Section 5 in which the forgoing numerical techniques are applied to four test problems, for which analytical solutions are available. Subsequently, the numerical study is extended to dynamic simulation of a semi-industrial seeded batch crystallizer as well as an industrial continuous crystallizer. Finally, the concluding remarks are outlined in Section 6.

2. Method of characteristics

In order to alleviate the deficiencies inherent in the discretized population balance equations, namely the numerical diffusion and instability problems in the vicinity of steep moving fronts, Kumar and Ramkrishna (1997) proposed a new approach that substantially enhances the accuracy of the discretized population balance equations. In this method, the convection term, i.e. $\partial(G(L,t)n(L,t))/\partial L$, is eliminated through the transformation of Eq. (1) to the following set of ordinary differential equations:

$$\frac{dL}{dt} = G(L,t), \tag{4}$$

$$\frac{dn(L,t)}{dt} = -n(L,t)\frac{dG(L,t)}{dL} + B(L,t) + Q(L,t,n), \tag{5}$$

where Eq. (4) expresses the movement of crystal cells and Eq. (5) governs the evolution of the crystal number density.

The mathematical procedure of transforming Eq. (1) to Eqs. (4) and (5) and solving the latter for a solution is known as the method of characteristics. This formulation implies that there exists unique characteristic curves along which information propagates. When the number density information moves along these pathlines, the convection term in the PBE disappears. This results in a significant improvement in the solution accuracy since the convection term is the prime source of numerical diffusion and instability.

Nonetheless, the presence of crystal nucleation poses a difficulty in the MOC. As the grid mesh moves with the growth rate, i.e. Eq. (4), a situation arises that some or all of the nuclei become smaller than the smallest crystal size. The nucleation term is therefore no longer represented accurately since the newly formed crystals cannot be placed in the first cell. To overcome this problem, a new cell of nuclei with zero crystal population should be added at regular time intervals. The number of cells and, consequently, the number of differential equations that have to be solved will however increase rapidly, making the method computationally too involved.

The main advantage of the numerical technique proposed by Kumar and Ramkrishna (1997) comes into play when the computational efficiency of the MOC is to be restored. In their approach, crystal cells are continually added at the smallest size to account for the crystal nucleation, whereas they are collapsed elsewhere to preserve the coarseness of the grid mesh. For any three size classes located such that $L_{i+1}/L_{i-1} < r_{critical}$, the ith class is collapsed and its population is assigned to the adjacent size classes while any two properties of the crystal size distribution is preserved. The crystal population fraction to be assigned to the $(i+1)$th and $(i-1)$th size classes should therefore satisfy

$$\eta_{i+1} = \frac{L_i^{\zeta} L_{i-1}^{v} - L_{i-1}^{v} L_{i-1}^{\zeta}}{L_{i+1}^{\zeta} L_{i-1}^{v} - L_{i+1}^{v} L_{i-1}^{\zeta}}, \tag{6}$$

$$\eta_{i-1} = \frac{L_i^{\zeta} L_{i+1}^{v} - L_{i-1}^{v} L_{i+1}^{\zeta}}{L_{i+1}^{v} L_{i-1}^{\zeta} - L_{i+1}^{\zeta} L_{i-1}^{v}}, \tag{7}$$

where the integer constants ζ and v are chosen such that the desired properties of the distribution are conserved.

It is evident that the primary feature of the MOC is efficient calculation of the desired properties of the population, rather than approximation of the continuous distribution on a suitably fine grid mesh. It is worth noting that this technique also has the merit of adapting geometric discretization schemes, which allows to tune the coarseness of the grid mesh. Nonetheless, there are some limitations in the method of characteristics that may restrict its use. The main difficulty concerns the trade-off that has to be sought between the choice of the time step, at which new crystal cells are added to account for the nucleation, and the computational time. Accurate preservation of the number of newly born crystals necessitates short time steps. To restore the computational efficiency, a relatively small number of cells is however desirable that conflicts with the requirement on the time step.

3. Finite volume methods

The finite volume methods involve discretization of the spatial variable domains and the use of piecewise functions to approximate the derivatives with respect to the spatial variables. The resulting set of ordinary differential equations, one for each grid point, is subsequently integrated over time along lines parallel to the time axis in the time–space domain.

The family of the finite volume methods encompasses a variety of numerical schemes that differ in the grid discretization and/or in the functions used to approximate the spatial derivatives. In these methods, the hyperbolic partial differential equation of Eq. (1) reduces to a semi-discrete equation per grid point that in the case of $Q(L,t,n)=0$, i.e. no inlet and outlet streams, is cast as

$$\frac{\partial n_i}{\partial t} + \frac{1}{\Delta L}([(Gn)_{L_i^+} - \mathbf{B}_{L_i^+}] - [(Gn)_{L_i^-} - \mathbf{B}_{L_i^-}]) = 0, \tag{8}$$

where $\mathbf{B}(L,t) = \int_0^L B(\xi,t)\,d\xi$. Note that $n_i(t)$ is a representative value for the number density in the cell i confined to $(L_{i-1/2}, L_{i+1/2})$; see the cell centered finite volume grid mesh depicted in Fig. 1. It is worth mentioning that in contrast with the finite difference methods, where the grid points constitute the computational nodes, in the finite volume methods the computations are done on the cell boundaries.

Calculation of Eq. (8) at each grid point requires values of the growth and nucleation rates as well as the number density on the cell boundaries. Though the growth and nucleation rates can be directly obtained form the kinetic expressions, estimation of the number density on the cell boundaries poses a difficulty in the foregoing

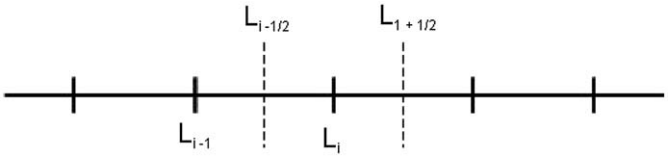

Fig. 1. Cell centered finite volume grid.

formulation. The approach by which the cell-face fluxes, i.e. $(Gn)_{L_i^+}$, are approximated mainly determines the accuracy of a finite volume method. The simplest interpolation formula that can be used to approximate the number density on each cell boundary is the upwind interpolation scheme. This approximation is equivalent to using a first order backward or forward difference approximation for the partial derivatives depending on the flow direction, i.e. crystal growth/dissolution. In the case of positive convection term, i.e. crystal growth, the first order interpolation scheme leads to

$$\frac{\partial n_i}{\partial t} + \frac{1}{\Delta L}([n_i G_{L_i^+} - \mathbf{B}_{L_i^+}] - [n_{i-1} G_{L_i^-} - \mathbf{B}_{L_i^-}]) = 0, \quad G(L) > 0. \tag{9}$$

When the nucleation only takes place at infinitesimally small crystal sizes, the flux across the inflow boundary, i.e. L_{1^-}, need not be approximated since $n_{1^-} = n_{in} = B_0/G|_{L_0}$.

The first order upwind finite volume method does not exhibit instability. It does however suffer from numerical diffusion unless a fine grid mesh is used. To circumvent the diffusion problem, higher order linear or quadratic interpolation schemes such as the piecewise polynomial interpolation formula (Qamar et al., 2006)

$$(Gn)_{L_i^+} = G_{L_i^+}\left(n_i + \frac{1+\kappa}{4}(n_{i+1} - n_i) + \frac{1-\kappa}{4}(n_i - n_{i-1})\right)$$
$$\kappa \in [-1, 1] \tag{10}$$

can be used. Eq. (10) yields a weighted blend between the central scheme and the fully one-sided scheme for different values of κ.

In spite of the fact that the higher order interpolation schemes suppress numerical diffusion to a large extent, they often result in oscillatory solutions (Ferziger and Peric, 1996). This problem can be rather easily tackled by limiting the flux across the cell boundaries with the aid of flux limiting functions. The latter functions ensure the monotonicity and prevent the occurrence of negative solutions. The formulation of the high order finite volume method with two of the most widely used flux limiting functions is given in Table 1, where r_i^+ and $\phi(r_i^+)$ denote the so-called upwind ratio of two consecutive solution gradients and the flux limiting function, respectively. These schemes provide second order accuracy in smooth regions and first order accuracy in the vicinity of discontinuities (Qamar and Warnecke, 2007). Note that the flux limiting functions cannot be applied to the left and right boundaries and, therefore, the first order upwind formulation should be used in the boundary cells. A thorough analysis of various flux limiting functions can be found in LeVeque (2002).

4. Finite element methods

The hyperbolic population balance equation can be solved in its continuous form using the finite element methods (FEMs). These techniques approximate the solution using piecewise low order polynomials that are locally nonzero and are, therefore, capable of capturing highly irregular solutions (Rigopoulos and Jones, 2003). Rawlings et al. (1993) indicated that the finite element methods normally possess modest computational burden, which facilitates their use in on-line control applications. The solution procedure pertaining

Table 1
The formulation of the high order finite volume method with various flux limiting functions in the case of $G(L) > 0$.

Koren (1993) ($\kappa = \frac{1}{3}$)
$((Gn)_{1/2} - \mathbf{B}_{1/2}) = G_{1/2} n_{in} - \mathbf{B}_{1/2}$
$((Gn)_{3/2} - \mathbf{B}_{3/2}) = \frac{1}{2}((G_{3/2} n_1 - \mathbf{B}_{3/2}) + (G_{3/2} n_2 - \mathbf{B}_{3/2}))$
$((Gn)_{L_i^+} - \mathbf{B}_{L_i^+}) = ((G_{L_i^+} n_i - \mathbf{B}_i) + \frac{1}{2}\phi(r_i^+)[(G_{L_i^+} n_i - \mathbf{B}_i) - (G_{L_i^+} n_{i-1} - \mathbf{B}_{i-1})]), \quad i = 1, \ldots, N-1$
$((Gn)_{N+1/2} - \mathbf{B}_{N+1/2}) = ((G_{N+1/2} n_N - \mathbf{B}_N) + \frac{1}{2}[(G_{N+1/2} n_N - \mathbf{B}_N) - (G_{N+1/2} n_{N-1} - \mathbf{B}_{N-1})])$
$r_i^+ = \frac{(G_{L_i^+} n_{i+1} - \mathbf{B}_{i+1}) - (G_{L_i^+} n_i - \mathbf{B}_i) + \varepsilon}{(G_{L_i^+} n_i - \mathbf{B}_i) - (G_{L_i^+} n_{i-1} - \mathbf{B}_{i-1}) + \varepsilon}$
$\phi(r_i^+) = \max(0, \min(2r_i^+, \min(\frac{1}{3} + \frac{2}{3} r_i^+, 2)))$
van Leer (1985) ($\kappa = -1$)
$((Gn)_{1/2} - \mathbf{B}_{1/2}) = G_{1/2} n_{in} - \mathbf{B}_{1/2}$
$((Gn)_{3/2} - \mathbf{B}_{3/2}) = \frac{1}{2}((G_{3/2} n_1 - \mathbf{B}_{3/2}) + (G_{3/2} n_2 - \mathbf{B}_{3/2}))$
$((Gn)_{L_i^+} - \mathbf{B}_{L_i^+}) = ((G_{L_i^+} n_i - \mathbf{B}_i) + \frac{1}{2}\phi(r_i^+)[(G_{L_i^+} n_{i+1} - \mathbf{B}_{i+1}) - (G_{L_i^+} n_i - \mathbf{B}_i)]), \quad i = 1, \ldots, N$
$r_i^+ = \frac{(G_{L_i^+} n_i - \mathbf{B}_i) - (G_{L_i^+} n_{i-1} - \mathbf{B}_{i-1}) + \varepsilon}{(G_{L_i^+} n_{i+1} - \mathbf{B}_{i+1}) - (G_{L_i^+} n_i - \mathbf{B}_i) + \varepsilon}$
$\phi(r_i^+) = \frac{\lvert r_i^+ \rvert + r_i^+}{1 + \lvert r_i^+ \rvert}$

to these methods can be generally summarized in the following steps:

1. The spatial domain is first divided into *ne* elements. The discretization scheme has to be selected carefully as it may have a profound impact on the accuracy and computational efficiency of the solution. In general, the discretization scheme should be tailored to the needs of the problem under consideration to achieve the best performance. For simultaneous nucleation and growth problems, geometric discretization schemes are often suited best since they provide a refined grid mesh at smaller size ranges to capture nucleation, while covering a broad range of size that is essential for large and size-dependent crystal growth rates.
2. The continuous number density function, i.e. $n(L,t)$, should then be approximated by a basis function. There is a variety of choices for the basis function depending on its order. The majority of FEM applications are favored to the higher order basis functions such as cubic splines (Gelbard and Seinfeld, 1978; Eyre et al., 1988), wavelets (Chen et al., 1996; Liu and Cameron, 2003), Chebyshev polynomials (Sandu and Borden, 2003) and high order Lagrange interpolation polynomials (Nicmanis and Hounslow, 1998; Alexopoulos et al., 2004; Roussos et al., 2005). Nonetheless, Mahoney and Ramkrishna (2002) and Rigopoulos and Jones (2003) used linear basis functions to solve the dynamic PBE. Though the FEM formulation using the linear basis functions is free from structural complexities inherent in the higher order functions and is therefore far easier to implement, fairly accurate results can only be obtained at the cost of large number of nodal points. The first order basis functions normally accommodate a much finer grid mesh in the same amount of computational time as the higher order basis functions since the latter functions require many more evaluations and interpolations for the same number of nodal points.
3. Next step is to formulate the weighted residual expressions. According to the formulation proposed by Finlayson (1980), the weighted residual expressions are obtained by multiplying the PBE

$$F(L,t) = \frac{\partial n(L,t)}{\partial t} + \frac{\partial (G(L,t) n(L,t))}{\partial L} - B(L,t) - Q(L,t,n) = 0 \qquad (11)$$

by a weight function. This results in the following weighted residual expression for each element

$$\int_{\Omega_e} \omega(L) F(L,t) = 0, \qquad (12)$$

which indicates that the function $F(L,t)$ is orthogonal to the weight function $\omega(L)$. Common choices for the weight function include Dirac delta functions, i.e. $\omega(L) = \delta(L - L_i)$, resulting in collocation on finite element methods (Gelbard and Seinfeld, 1978; Alexopoulos et al., 2004; Rigopoulos and Jones, 2003) and the basis functions themselves, leading to Galerkin's techniques (Chen et al., 1996; Mahoney and Ramkrishna, 2002; Roussos et al., 2005). In the collocation methods, Eq. (12) should be evaluated at the nodal points, whereas in the latter methods it has to be integrated over each
element; implying that the Galerkin's techniques are computationally more expensive. A comparative analysis of various integration formulas used to solve the Galerkin's methods can be found in Roussos et al. (2005).
4. The resulting set of stiff nonlinear algebraic differential equations is integrated in time.

In the application of FEMs to processes in which nucleation only occurs at infinitesimally small crystal sizes, handling of the nucleation term requires special care. Since the nucleation is implemented as a point source at the first nodal point, the common continuous non-singular basis functions cannot resolve the pulse-like nucleation term. Hence, it is assumed that the nucleation spreads over a specified size range (Rigopoulos and Jones, 2003; Alexopoulos and Kiparissides, 2005). This approach may however severely suffer from numerical problems as the number density at size zero possesses two values corresponding to the initial distribution and the nucleation rate. This incompatibility between the initial condition, i.e. initial distribution, and the boundary condition, i.e. nucleation rate, gives rise to moving discontinuities in the numerical solution that can be dealt with by means of discontinuous finite element methods (Mahoney and Ramkrishna, 2002).

Another numerical problem that is commonly encountered in the finite element methods arises from the convective nature of the PBE. The basis functions are evaluated at interior points of each element. As a result, information flows to the nodal points from both ends of the element. However, this mechanism is not entirely valid for the numerical solution of the PBE due to the convective nature of the crystal growth phenomenon, i.e. crystals only grow in one direction from smaller to larger sizes. The numerical instability problems that arise from the foregoing shortcoming of the FEM formulation may be alleviated by adopting a geometric grid discretization scheme and tuning its resolution. Another common practice to suppress this numerical problem is to include an artificial diffusion term to dampen the oscillations that appear in distributions with steep moving fronts (Alexopoulos et al., 2004; Roussos et al., 2005). The latter approach might be more appealing as the growth problems are best solved on a uniform grid mesh.

In this study, both the orthogonal collocation on finite elements (OCFE) and the Galerkin's on finite element method (GFEM) are studied. The continuous number density function over each element is approximated by

$$n_e(L,t) = \sum_{j=1}^{np} n_j^e(t) \varphi_j^e(L), \qquad (13)$$

where np and $\varphi_j^e(L)$ denote the nodal points and the basis functions, respectively. In order to investigate the effect of the basis functions on performance of either of the finite element methods, high order

Lagrange interpolation polynomials

$$\varphi_j^e(L) = \prod_{j=1,\, j\neq i}^{nc+1} \frac{(L - L_j^e)}{(L_i^e - L_j^e)} \tag{14}$$

as well as the linear basis function

$$\varphi(L)_{[j-1,j]} = \left(\frac{L - L_{j-1}}{L_j - L_{j-1}}, \frac{L_j - L}{L_j - L_{j-1}} \right) \tag{15}$$

are used to approximate the number density function. In the latter case, the number density over an element is expressed as

$$n(L,t)_{[j-1,j]} = n(L_{j-1},t)\frac{L - L_{j-1}}{L_j - L_{j-1}} + n(L_j,t)\frac{L_j - L}{L_j - L_{j-1}}. \tag{16}$$

5. Results and discussion

The method of characteristics, the finite volume methods and the finite element methods are used to solve various crystallization processes undergoing simultaneous nucleation and growth. The following features of the solution methods are thoroughly investigated:

- the effect of cell elimination in the method of characteristics,
- the impact of the interpolation formula in the finite volume methods and
- the choice of the basis function and the weight function in the finite element methods.

In order to validate the numerical solution methods, they are first applied to four test problems with constant supersaturation, for which analytical solutions are available. Besides examining the implementation-related issues, the performance of the solution methods is assessed with respect to their numerical accuracy and computational efficiency. The accuracy of the numerical techniques is quantified in terms of the errors in the zeroth and the third moments of the number density distribution

$$m_i - \mathtt{error} = |(m_i)_{analytical} - (m_i)_{numerical}|, \quad i = 0, 3. \tag{17}$$

The zeroth and the third moments defined as

$$m_i = \int_{L_{\min}}^{L_{\max}} n(L,t) L^i \, dL, \quad i = 0, 3 \tag{18}$$

correspond to the total number of crystals and the total crystal volume, respectively. The integrals are evaluated using the trapezoidal rule.

Numerical simulation of real crystallization systems is further complicated by the nonlinear dependence of crystallization phenomena on process variables, e.g. temperature, solute concentration, etc. This study is therefore extended to dynamic simulation of a semi-industrial seeded batch crystallizer and an industrial continuous crystallizer. The mode of operation of the crystallization processes is chosen such that the population balance model of the systems under consideration can also be solved analytically to be able to analyze the numerical accuracy of the solution methods for real case studies. The main feature that makes the latter case studies particularly interesting is their time-varying supersaturation profile, which enables a more realistic comparison of the various solution methods.

All the test problems presented in this section are implemented in MATLAB (version 7.5.0.342), where the initial value problems are solved using the Euler integration method. The reported CPU times correspond to the Microsoft Windows XP (Professional) operating system running on a Genuine Intel(R) T2050 @1.60 GHz processor with 1 GB RAM.

5.1. Test problem 1: size-independent growth of a pre-existing distribution

The first test problem concerns size-independent growth of a complex initial distribution. Though in practice initial distributions are normally of Gaussian type, under certain circumstances, for instance burst of infinitesimally crystals after insertion of seeds to a supersaturated solution, they can exhibit extremely sharp discontinuities. This test problem, taken from Qamar et al. (2006), allows us to analyze how the solution methods deal with the discontinuities of different type.

The initial number density, distributed over an equidistant grid mesh from $L_{\min} = 0\,\mu m$ to $L_{\max} = 100\,\mu m$, is defined as

$$n(L,0) = \begin{cases} 0.0 & \text{if } L \leq 2.0, \\ 10^9 & \text{if } 2.0 < L \leq 10.0, \\ 0.0 & \text{if } 10.0 < L \leq 18.0, \\ 10^9 \cos^2(\pi(L-26)/64) & \text{if } 18.0 < L \leq 34.0, \\ 0.0 & \text{if } 34.0 < L \leq 42.0, \\ 10^9 (1 - (L-50)^2/64))^{0.5} & \text{if } 42.0 < L \leq 58.0, \\ 0.0 & \text{if } 58.0 < L \leq 66.0, \\ 10^9 \exp(-(L-70)^2/\Delta L^2) & \text{if } 66.0 < L \leq 74.0, \\ 0.0 & \text{if } L > 74.0, \end{cases} \tag{19}$$

where $\Delta L = (L_{\max} - L_{\min})/(N-1)$ and N denotes the number of grid points. The analytical solution to this problem is

$$n(L,t) = n_0(L - Gt), \tag{20}$$

which implies that the initial distribution is shifted for a distance of Gt. G is assumed to be $0.1\,\mu m/s$.

Fig. 2 presents the comparison of various numerical schemes after integration time of 60 s. The errors and computational times corresponding to the integration time step, dt, of 0.1 s are listed in Table 2. Clearly, the method of characteristics provides the most accurate results. On the contrary, results of the first order upwind finite volume method are very diffusive. This problem is to a large extent alleviated in the high order finite volume methods combined with flux limiting functions. Note that it is vital to use the flux limiting function to suppress the oscillations inherent in the high order finite volume methods and, consequently, circumvent negative solutions; see Fig. 2(c). The choice of the flux limiting function, namely van Leer (1985) and Koren (1993), barely affects the accuracy and computational burden of the high order finite volume method.

The orthogonal collocation method and the Galerkin's method, on the other hand, provide less promising results. The orthogonal collocation with the linear basis function yields reasonable predictions, comparable to the first order upwind finite volume method in terms of the numerical accuracy. This is due to the fact that this method consists of collocation on linear elements with an upwind propagation of growth to ensure the stability of the scheme. On the contrary, the orthogonal collocation and Galerkin's methods with the Lagrange basis function, which do no exploit such stability condition, display oscillatory behavior. This problem can be overcome to a certain extent either by employing the so-called artificial diffusion term or increasing the number of elements as demonstrated in Fig. 2(e) and (f), respectively. In the latter figure *ne* represents the number of finite elements, whereas *nc* is the degree of the Lagrange interpolation polynomial. Even though increasing the number of elements slightly improves the results, the Galerkin's method fails to fully suppress the oscillations with reasonable number of elements. The finite element methods are less attractive than the high order finite volume methods with flux limiting functions even in terms of the computational efficiency.

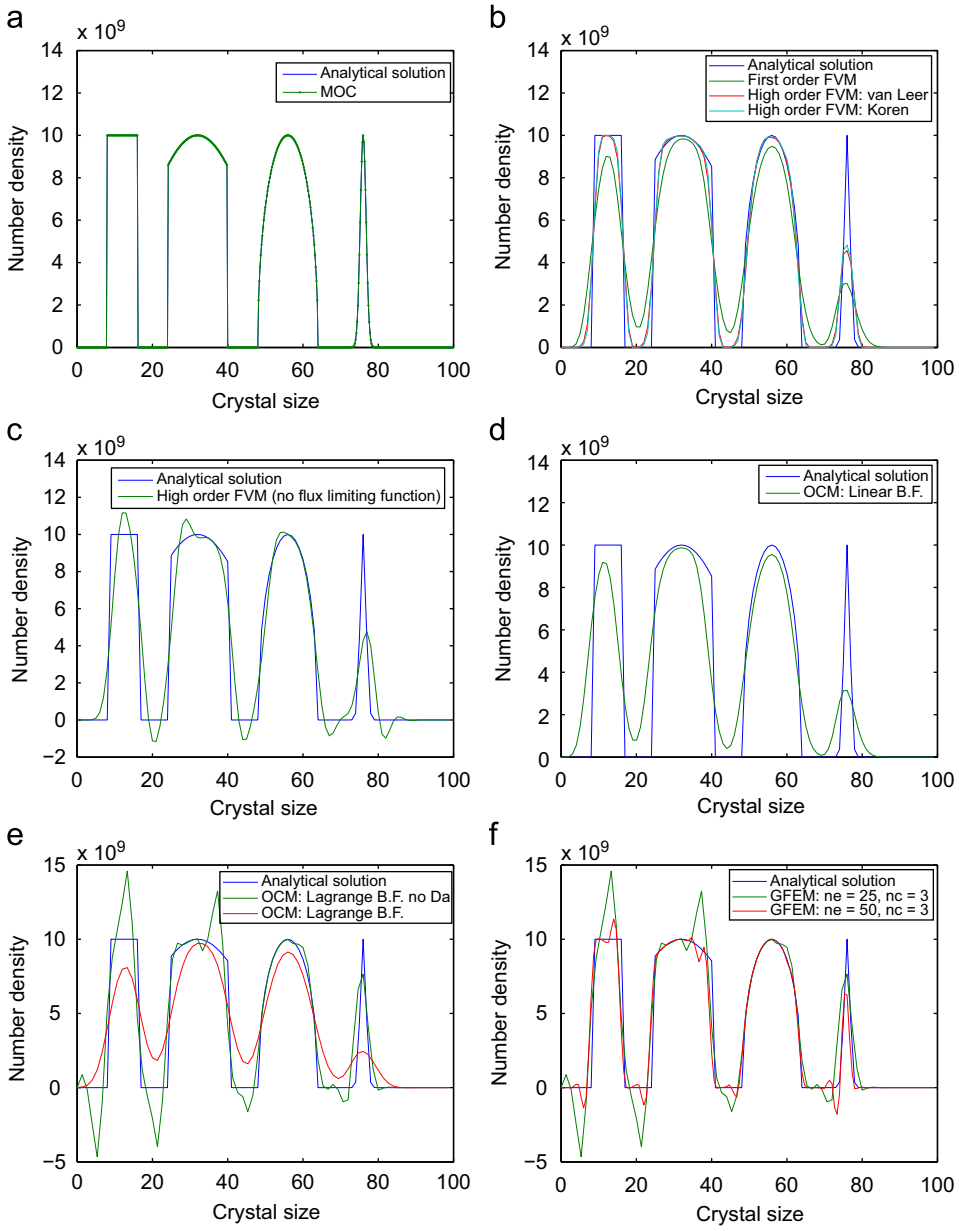

Fig. 2. Comparison of analytical and numerical results for test problem 1. (a) Method of characteristics. (b) Finite volume methods. (c) High order finite volume method (no flux limiting function). (d) Orthogonal collocation (linear basis function). (e) Orthogonal collocation (Lagrange basis function). (f) Galerkin on finite element (Lagrange basis function).

Table 2
Errors and computational times of test problem 1 ($t_{end} = 60$ s and $dt = 0.1$ s).

	Ngrids	CPU time (s)	m_0 error (%)	m_3 error (%)
MOC	100	0.21	0.12	0.15
First order FVM	100	0.16	3.70	0.50
High order FVM: van Leer	100	0.16	1.72	0.26
High order FVM: Koren	100	0.18	1.72	0.22
OCM: linear B.F.	100	0.24	3.95	0.90
OCM: Lagrange B.F.	75	0.40	5.28	2.63

5.2. Test problem 2: nucleation and size-independent growth from a clear solution

This test problem involves simultaneous nucleation and size-independent growth from a clear solution, i.e. unseeded batch crystallization. According to Hounslow et al. (1988), for this case the population balance equation becomes

$$n(L,t) = \frac{B_0}{G} u\left(t - \frac{L}{G}\right), \tag{21}$$

where u is the unit step function. It follows that the number density in the ith interval is

$$n_i = \begin{cases} \dfrac{\Delta L_i B_0}{G} & L_{i+1} \le tG, \\ \dfrac{B_0(tG - L_i)}{G} & L_{i+1} \ge tG > L_i, \\ 0 & L_i > tG. \end{cases} \tag{22}$$

As the solution is a discontinuity that moves with time, this is an ill-conditioned problem exhibiting severe numerical instabilities. Here, B_0 and G are both taken as 1.0.

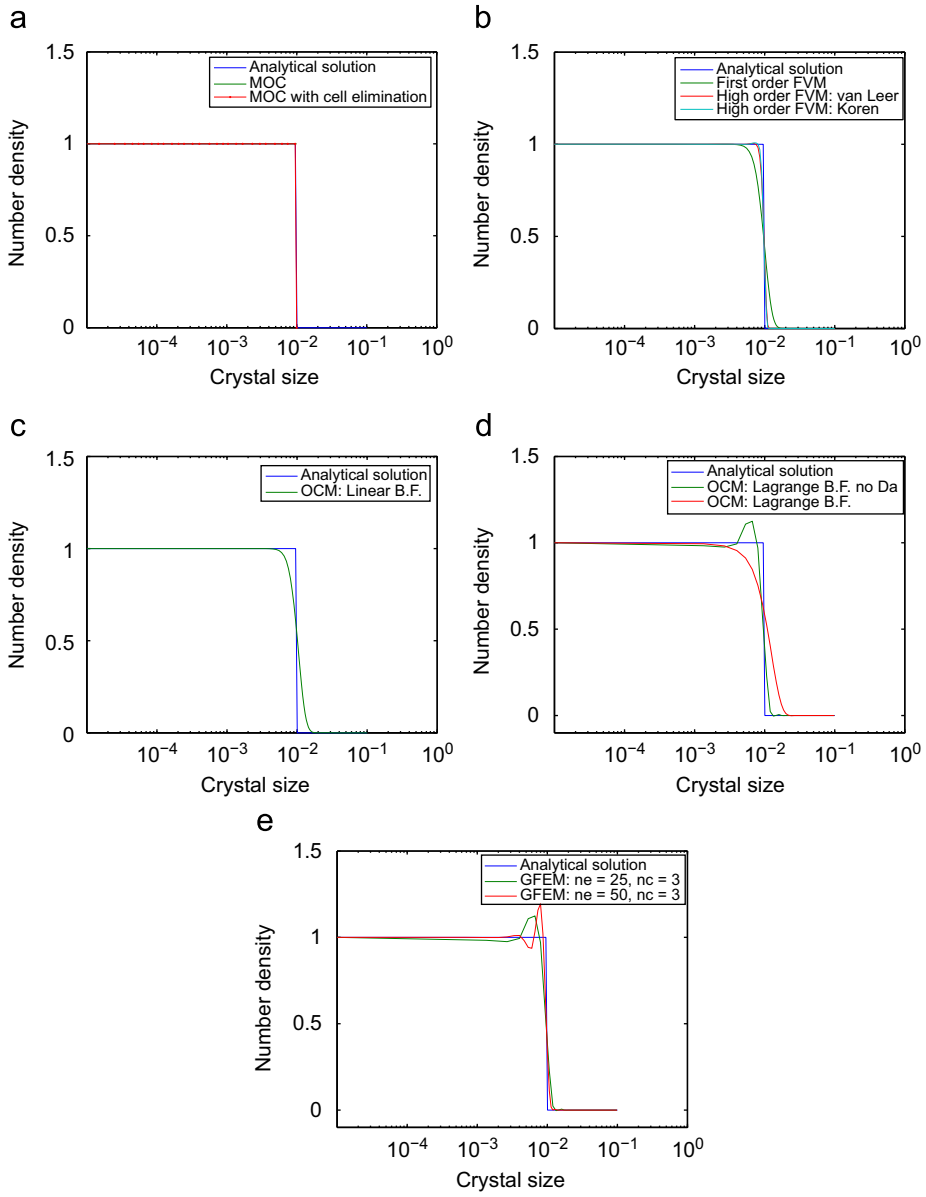

Fig. 3. Comparison of analytical and numerical results for test problem 2. (a) Method of characteristics. (b) Finite volume methods. (c) Orthogonal collocation (linear basis function). (d) Orthogonal collocation (Lagrange basis function). (e) Galerkin on finite element (Lagrange basis function).

The numerical and analytical results are depicted in Fig. 3. Yet again the method of characteristics gives the best numerical accuracy. This is however obtained at the cost of much higher computational time as opposed to the other numerical techniques. An effective way to restore the computational efficiency of the method of characteristics without jeopardizing its accuracy is to collapse the redundant cells and assign their population to the adjacent cells such that any two desired properties of the distribution are conserved. This strategy drastically reduces the computational burden, while preserving the numerical accuracy of the solution rather well; see Table 3.

Fig. 3(b) reveals that the first order upwind as well as the high order finite volume methods with flux limiting functions yield stable results. The accuracy of the solution at the steep moving front is however impaired due to the numerical diffusion. This effect can be partially mitigated, in particular for the first order upwind finite volume method, by the use of a finer grid mesh; see Table 3. Since the orthogonal collocation method with the linear basis function is stable, its numerical accuracy can also be improved by increasing the number of elements; obviously at the expense of higher computational time. The orthogonal collocation and Galerkin's methods with the Lagrange basis function, on the other hand, pose an additional difficulty as they are not numerically stable. Likewise the previous test problem, their stability is restored fairly well either by introducing the artificial diffusion term or increasing the number of elements. Table 3 indicates that the finite element methods are much less numerically accurate than the other techniques.

5.3. Test problem 3: nucleation and size-independent growth of a pre-existing distribution

The third test problem consists of crystal nucleation at infinitesimally small sizes and size-independent growth. The square step

Table 3
Errors and computational times of test problem 2: effect of discretization on the accuracy of the calculated moments ($t_{end} = 0.01$ s and $dt = 10^{-5}$ s).

	Ngrids	CPU time (s)	m_0 error (%)	m_3 error (%)
MOC	1000	69.62	0.07	0.13
MOC: cell elimination	28	0.61	0.10	0.41
First order FVM	100	0.89	4.19	46.74
	200	2.15	1.69	29.26
High order FVM: van Leer	100	0.88	1.19	3.75
	200	2.22	0.69	0.51
High order FVM: Koren	100	0.90	1.19	3.66
	200	2.15	0.69	0.55
OCM: linear B.F.	100	0.97	8.71	49.05
	200	2.22	4.21	31.93
OCM: Lagrange B.F.	75	1.30	9.11	37.49
GFEM: Lagrange B.F.	150	2.83	3.04	26.33

initial number density distribution is

$$n(L,0) = \begin{cases} 100 & 0.4 \le L \le 0.6, \\ 0.01 & \text{elsewhere}, \end{cases} \tag{23}$$

where the crystal size range is $0 \le L \le 2.0$. Assuming that the nucleation term has the following dependence on time

$$B_0 = 100 + 10^6 \exp(-10^4 (t - 0.215)^2), \tag{24}$$

the analytical solution to this problem is expressed as (Lim et al., 2002)

$$n(L,t) = \begin{cases} 100 + 10^6 \exp(-10^4 \\ \quad \times ((Gt - L) - 0.215)^2) & 0.0 \le L \le Gt, \\ 100 & 0.4 \le L - Gt \le 0.6, \\ 0.01 & \text{elsewhere}. \end{cases} \tag{25}$$

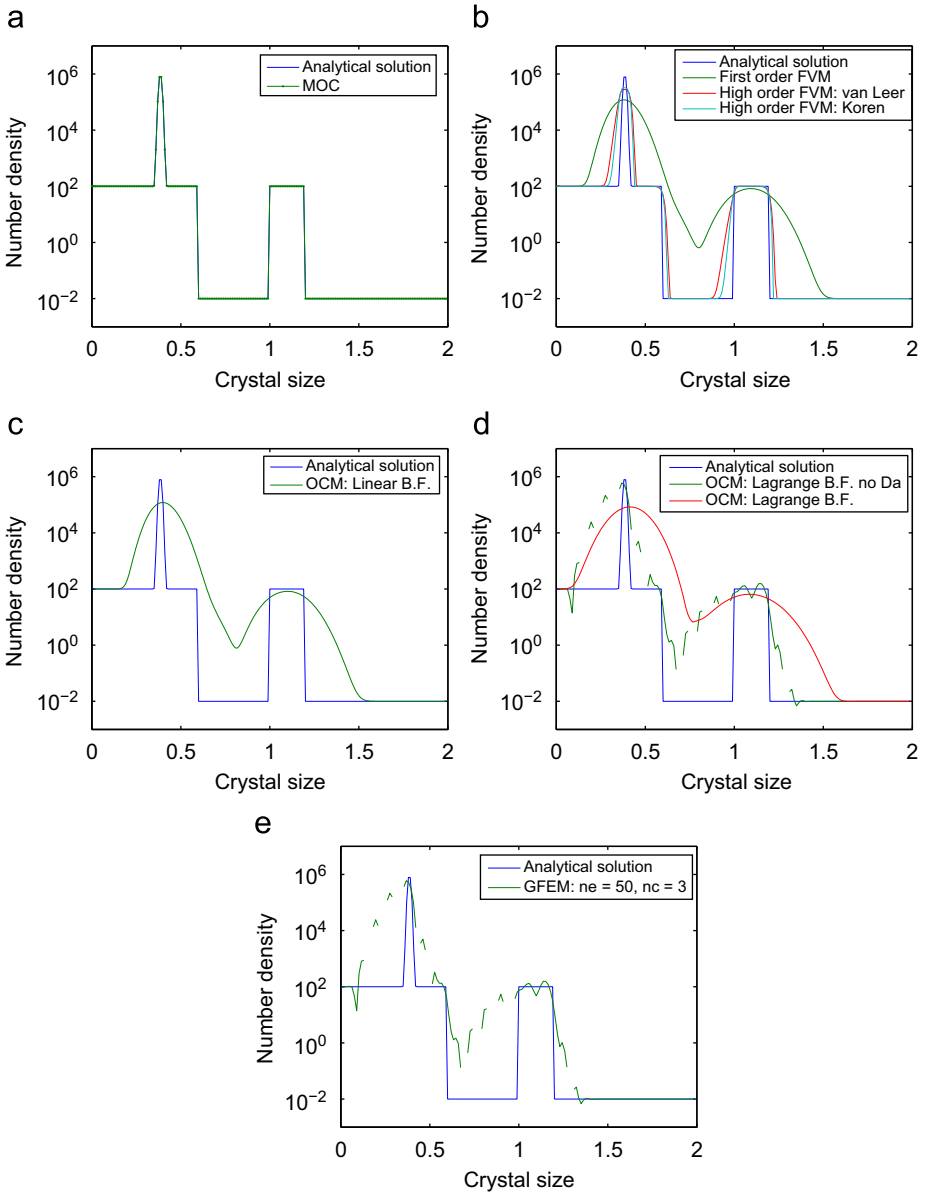

Fig. 4. Comparison of analytical and numerical results for test problem 3. (a) Method of characteristics. (b) Finite volume methods. (c) Orthogonal collocation (linear basis function). (d) Orthogonal collocation (Lagrange basis function). (e) Galerkin on finite element (Lagrange basis function).

Table 4
Errors and computational times of test problem 3 ($t_{end} = 0.6$ s and $dt = 10^{-3}$ s).

	Ngrids	CPU time (s)	m_0 error (%)	m_3 error (%)
MOC	200	1.14	0.01	0.82
First order FVM	200	0.72	2.34	6.13
High order FVM: van Leer	200	0.75	1.63	1.15
High order FVM: Koren	200	0.75	1.54	1.41
OCM: linear B.F.	200	0.76	2.95	9.67
OCM: Lagrange B.F.	150	1.11	3.28	14.43

Table 5
The parameters of test problem 4.

B_0	G_0	N_0	L_0	$L_{0,n}$
10^5	1	10	0.01	0.001

Eq. (25) implies that the solution comprises of a discontinuous shock and a narrow wave, originated from the seed distribution and the nucleation, respectively, that move with time. Here, G is considered to be 1.0.

The numerical results are shown in Fig. 4. As can be seen, the method of characteristics solves the problem very well. Application of the first order upwind finite volume method and the orthogonal collocation method with the linear basis function lead to very diffusive solutions, whereas the high order finite volume methods with flux limiting functions resolve the discontinuous profiles rather well; see the errors listed in Table 4. Interestingly, neither the orthogonal collocation method nor the Galerkin's method with the Lagrange basis function can give reasonable numerical results. Fig. 4(d) and (e) demonstrate that these methods suffer from severe oscillation. Qamar et al. (2006) also reported that PARSIVAL, which is a commercial package using hp-Galerkin's finite element method as its core scheme (Wulkow et al., 2001), gives highly oscillatory solution for this problem.

5.4. Test problem 4: exponential nucleation and size-independent growth of a pre-existing distribution

This test problem concerns a process with exponential nucleation

$$\mathbf{B}(L) = \frac{B_0}{L_{0,n}} \exp\left(-\frac{L}{L_{0,n}}\right) \tag{26}$$

and size-independent growth, i.e. $G = G_0$. The process starts with a pre-existing population of the form

$$n_0(L) = \frac{N_0}{L_0} \exp\left(-\frac{L}{L_0}\right). \tag{27}$$

According to Kumar and Ramkrishna (1997), the analytical solution to this problem is expressed as

$$n(t,L) = n_0(L - Gt) + \frac{B_0}{G_0}\left[\exp\left(-\frac{L_{low}}{L_{0,n}}\right) - \exp\left(-\frac{L}{L_{0,n}}\right)\right],$$
$$L_{low} = \max(L_0, L - G_0 t), \tag{28}$$

where the parameters are listed in Table 5. This problem is more complex than the previous test problem in that the new crystals are born in all size classes, i.e. crystal cells, rather than only the first one.

To solve this problem, the spatial domain is partitioned using the geometric discretization scheme

$$L_{1/2} = L_{\min}, \quad L_{i+1/2} = L_{\min} + 2^{(i-N)/q}(L_{\max} - L_{\min}), \quad i = 1, \ldots, N, \tag{29}$$

where N and q are taken as 100 and 7, respectively. The geometric scheme enables one to better capture the initial part of the number density distribution with sufficient number of cells, while avoiding a very fine grid mesh that may be detrimental to the computational efficiency of the solution method.

The numerical results are compared with the analytical solution in Fig. 5. Though numerical predictions of the method of characteristics are in excellent agreement with the analytical solution, this approach is much more computationally involved than the other methods. This is due to the fact that at each integration time step a cell is added to account for the newly created crystals. As a result, the number of cells rises from 100 to 1100 given that $t_{end} = 10^{-2}$ s and $dt = 10^{-5}$ s. The redundant cells are therefore eliminated, while preserving two desired moments of the number distribution. As shown in Table 6, in spite of the significant improvement in the computational efficiency, the accuracy of the numerical results remains almost intact. Likewise the previous case studies, the high order finite volume methods with flux limiting functions exhibit superior performance to the first order upwind finite volume method and the collocation method with the linear basis function. The finite element methods with the Lagrange basis function yet again fail to capture the steep moving front as depicted in Fig. 5(d) and (e).

5.5. Semi-industrial seeded batch crystallizer

The numerical solution methods are used to simulate a semi-industrial 75-l draft tube crystallizer (Mesbah et al., 2008). The process at hand is seeded fed-batch evaporative crystallization of an ammonium sulphate–water system. The initial seeds possess a log-normal distribution

$$n(L,0) = \left(\frac{\varepsilon}{K_v L^3}\right) \frac{1}{\ln(\sigma_{g,1})\sqrt{2\pi}L} \exp\left(-\frac{\left(\ln\left(\frac{L}{L_{0,g1}}\right)\right)^2}{2(\ln(\sigma_{g,1}))^2}\right), \tag{30}$$

which is discretized by using an equidistant grid mesh comprised of 1200 crystal cells.

The empirical expressions realized to model the crystal nucleation at infinitesimally small sizes and the size-independent crystal growth rate are

$$B_0 = k_b m_3 G, \tag{31}$$
$$G = k_g (C - C^*)^g, \tag{32}$$

respectively. It is well evident that the nucleation and crystal growth rates are nonlinear functions of the solute concentration that may further complicate the solution of the population balance equation.

The analytical solution to the PBE, i.e. Eq. (2), with the given power law kinetic expressions can be obtained by multiplying Eq. (2) by $L^i dL$ and, subsequently, integrating over the entire crystal size domain. This results in the following set of ordinary differential equations known as the moment model

$$\frac{dm_0}{dt} = B_0 - \frac{m_0 Q_p}{V},$$
$$\frac{dm_i}{dt} = iGm_{i-1} - \frac{m_i Q_p}{V}, \quad i = 1, \ldots, 4. \tag{33}$$

Eq. (33) suggests that the analytical solution to this crystallization problem consists of the first five leading moments of the crystal size distribution. As the kinetic expressions are dependent on the solute concentration, the solute concentration balance

$$\frac{dC}{dt} = \frac{\frac{Q_p(C^* - C)}{V} + 3K_v G m_2 (k_1 + C)}{1 - K_v m_3} + \frac{k_2 H_{in}}{1 - K_v m_3} \tag{34}$$

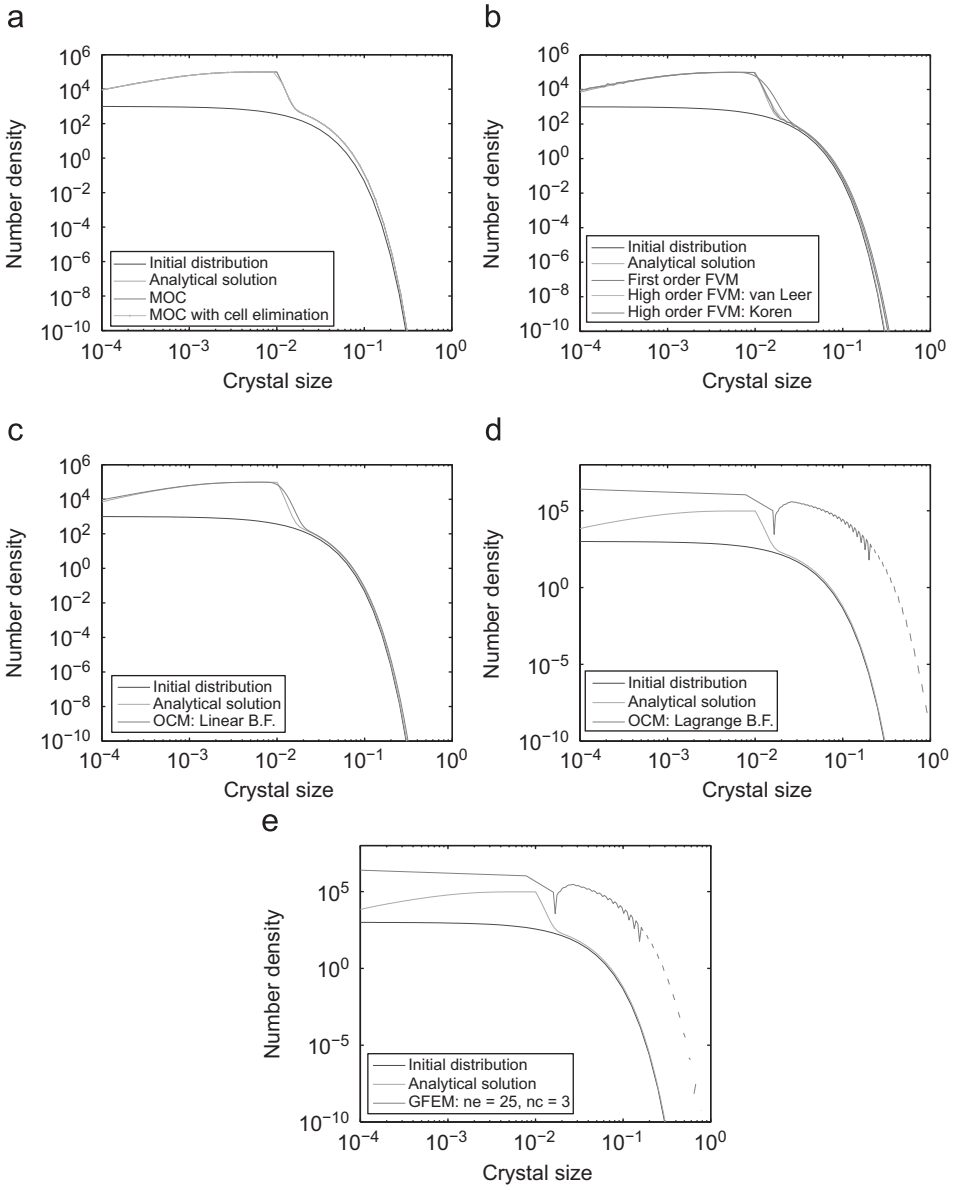

Fig. 5. Comparison of analytical and numerical results for test problem 4. (a) Method of characteristics. (b) Finite volume methods. (c) Orthogonal collocation (linear basis function). (d) Orthogonal collocation (Lagrange basis function). (e) Galerkin on finite element (Lagrange basis function).

Table 6
Errors and computational times of test problem 4 ($t_{end} = 10^{-2}$ s and $dt = 10^{-5}$ s).

	Ngrids	CPU time (s)	m_0 error (%)	m_3 error (%)
MOC	1100	35.18	1.20	0.46
MOC: Cell elimination	49	1.85	1.22	0.48
First order FVM	100	0.93	11.39	19.02
High order FVM: van Leer	100	1.08	3.69	3.37
High order FVM: Koren	100	1.06	3.69	3.59
OCM: Linear B.F.	200	2.30	5.10	17.92

with constant coefficients

$$k_1 = \frac{H_v C^*}{H_v - H_L}\left(\frac{\rho_c}{\rho_L} - 1 + \frac{\rho_L H_L - \rho_c H_c}{\rho_L H_v}\right) - \frac{\rho_c}{\rho_L}, \tag{35}$$

$$k_2 = \frac{C^*}{V\rho_L(H_v - H_L)} \tag{36}$$

should also be coupled with the set of ordinary differential equations given in Eq. (33). The parameters of the moment model are listed in Table 7.

The population balance equation that represents the semi-industrial crystallization process under consideration is solved by the method of characteristics, the finite volume methods of different order and the orthogonal collocation as well as the Galerkin's finite

Table 7
Parameters of the batch crystallization model.

Symbol	Parameter	Value	Unit
C^*	Equilibrium concentration	0.46	$kg_{solute}/kg_{solution}$
g	Growth rate exponent	1.0	–
H_c	Specific enthalpy of crystals	60.75	kJ/kg
H_L	Specific enthalpy of liquid	69.86	kJ/kg
H_v	Specific enthalpy of vapor	2.59×10^3	kJ/kg
K_v	Volumetric shape factor	0.43	–
k_b	Nucleation rate constant	1.02×10^{14}	$\#/m^4$
k_g	Growth rate constant	7.50×10^{-5}	m/s
$L_{0,g1}$	Location parameter of distribution	310.3×10^{-6}	m
Q_p	Product flow rate	1.73×10^{-6}	m^3/s
V	Crystallizer volume	7.50×10^{-2}	m^3
ρ_c	Density of crystals	1767.35	kg/m^3
ρ_L	Density of saturated solution	1248.93	kg/m^3
ε	Crystal fraction	0.038	–
$\sigma_{g,1}$	Spread parameter of distribution	1.51	–

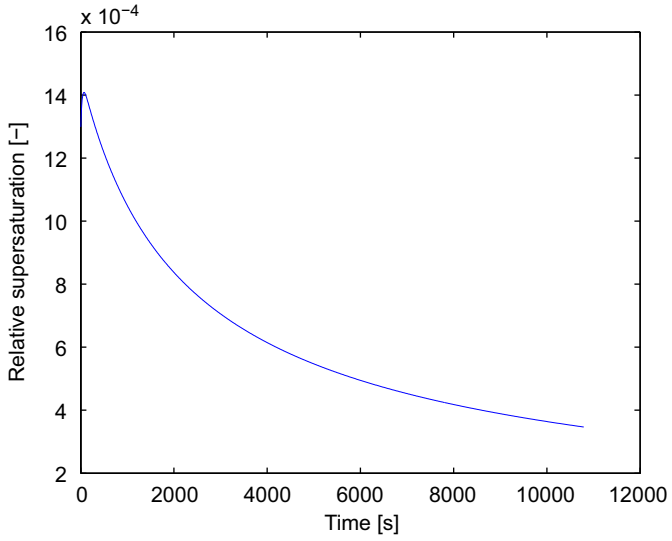

Fig. 6. Supersaturation profile throughout the batch.

element methods using different basis functions. It is worth noting that three variants of the method of characteristics formulation are considered:

- case 1, without crystal cell elimination,
- case 2, in which only the last crystal cell is eliminated and
- case 3, where the cells for which $L_{i+1}/L_{i-1} < r_{critical} = 1.05$ are eliminated.

Fig. 6 shows the supersaturation profile throughout the batch process of 10800 s. The crystal size distributions corresponding to different time instants of the batch process are depicted in Fig. 7. As listed in Table 8, cell elimination drastically reduces the computational effort of the method of characteristics while the accuracy of the numerical results is preserved rather well. It is evident that the elimination of the last crystal cell, i.e. case 2, only slightly deteriorates the numerical accuracy, whereas the loss of accuracy is more pronounced in case 3, particularly in the zeroth and first moments. It should be mentioned that the choice of $r_{critical}$ has to be made carefully since large values of $r_{critical}$ may substantially worsen the accuracy of the numerical results.

Numerical results of the first order upwind and the high order finite volume method with van Leer flux limiting function are depicted in Fig. 7(b) and (c), respectively. It is shown that the crystal size distributions simulated by the first order upwind finite volume method considerably suffer from the numerical diffusion problem, while the high order finite volume method with the flux limiting function exhibits this problem to a much less extent. As a result, the numerical accuracy of the latter method is significantly better than that of the first order upwind finite volume method, especially in the higher moments, whereas all the variants of the finite volume method possess almost the same computational efficiency; see Table 9. The high order finite volume method with flux limiting function is therefore considered to be superior to the first order upwind method. Furthermore, the numerical accuracy of the high order finite volume method with flux limiting function is comparable to that of the method of characteristics in the case that the redundant crystal cells are eliminated, while it is computationally less expensive. The lower computational burden of the high order finite volume method with flux limiting function can be attributed to their Jacobian matrix consisting of $Ngrids \times Ngrids$ entries, where $Ngrids$ denotes the number of grid points. The method of characteristics however has a $2Ngrids \times 2Ngrids$ Jacobian matrix since the PBE translates to two ordinary differential equations for each grid point; see Eqs. (4) and (5). The method of characteristics is therefore more computation intensive.

Fig. 7(d) reveals that the orthogonal collocation method with the linear basis function suffers from the numerical diffusion problem, even more severely than the first order upwind finite volume method; see Table 10. Fig. 7(e) and (f), on the other hand, suggest that the orthogonal collocation and the Galerkin's methods with the Lagrange basis function are almost free from the numerical diffusion problem. They do however pose oscillatory behavior that can to a large extent be alleviated by increasing the number of elements at the cost of higher computational burden. As shown in Table 10, the finite element methods using the Lagrange basis function exhibit larger computational burden than the orthogonal collocation method with the linear basis function.

5.6. Industrial continuous crystallizer

The solution methods are also applied to simulate continuous evaporative crystallization of an ammonium sulphate-water system in a 1100-l draft tube baffle crystallizer (Motz et al., 2003). For the continuous well-mixed crystallizer equipped with a fines removal system, the general population balance equation given in Eq. (1) can be rewritten as

$$\frac{\partial n(L,t)}{\partial t} + \frac{\partial (G(L,t)n(L,t))}{\partial L} = -\frac{n(L,t)}{\tau} - h(L)\frac{n(L,t)}{\tau_f} \tag{37}$$

assuming that the inlet flow to the crystallizer is crystal free. In Eq. (37), τ and τ_f are the mean residence times of the dispersed phase in the crystallizer and the fines removal section, respectively, whereas $h(L)$ denotes the crystal classification function. The boundary condition of the PBE is expressed by Eq. (3).

Likewise the previous case study, a time-varying supersaturation profile computed from the solute concentration balance, i.e. Eq. (34), governs the nucleation and crystal growth rates throughout the process. The power law relation of Eq. (32) determines the crystal growth rate, whereas the empirical secondary nucleation expression proposed by Ottens et al. (1972)

$$B_0 = k_b \int_{L_{SN}}^{\infty} n(L,t)L^3\, dL \tag{38}$$

is used to model the nucleation process due to the crystal-impeller attrition. The initial conditions of the process under consideration are dictated by an initial seed distribution; see Eq. (30).

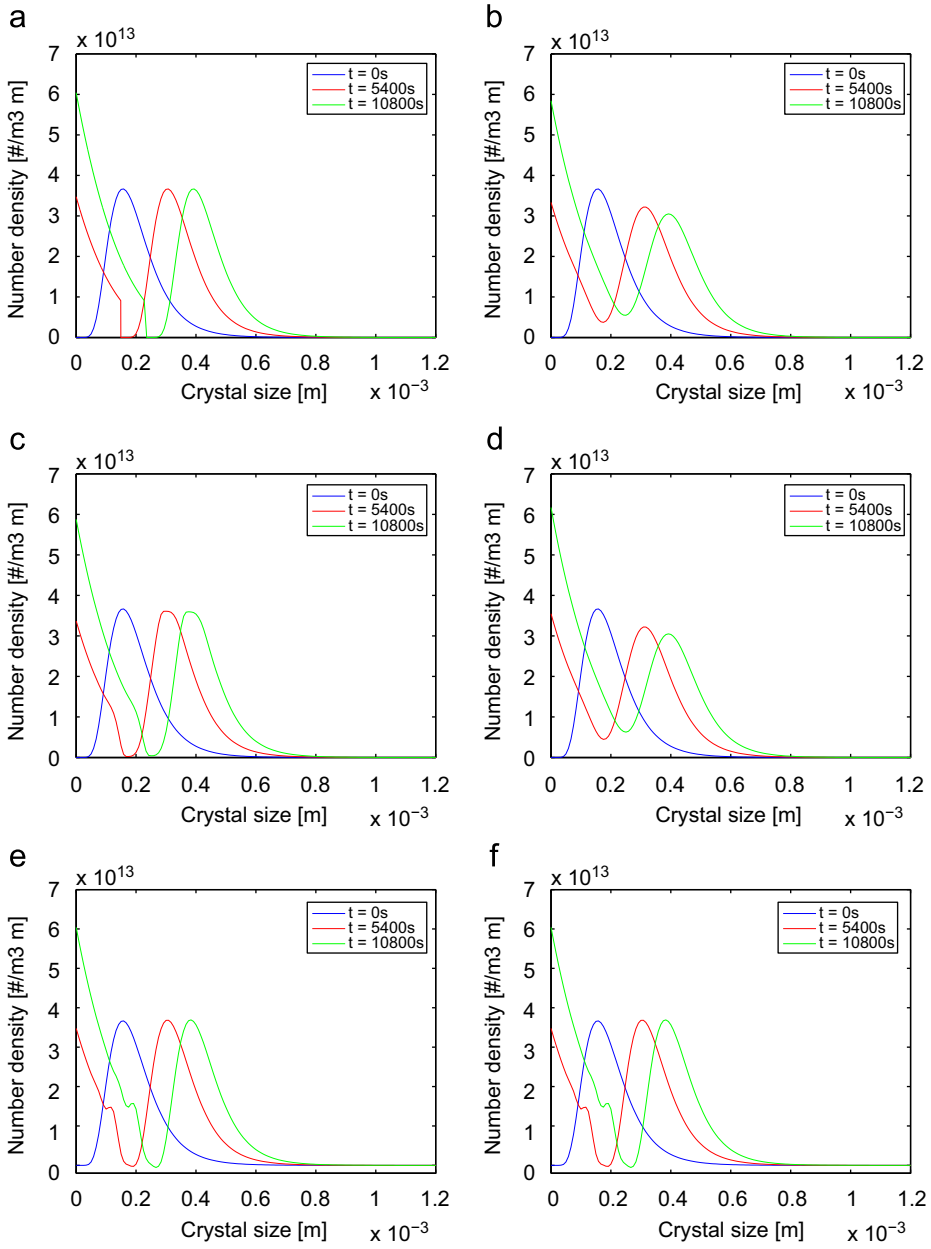

Fig. 7. Crystal size distribution at different time instants during the batch. (a) Method of characteristics (case 2). (b) First order FVM. (c) High order FVM: van Leer. (d) Orthogonal collocation (linear basis function). (e) Orthogonal collocation (Lagrange basis function). (f) Galerkin on finite element (Lagrange basis function).

In order to be able to analytically solve Eq. (37) for the steady state condition, the ideal function

$$h(L) = \begin{cases} 1 & \text{if } L < L_f, \\ 0 & \text{if } L \geq L_f \end{cases} \tag{39}$$

is considered to determine the crystal classification in the fines removal flow. According to Randolph and Larson (1988), under this assumption the number density at the steady state is

$$n(L) = \begin{cases} n(0)\exp\left(-\dfrac{RL}{G_{ss}\tau}\right) & \text{if } L < L_f, \\ n(0)\exp\left(-\dfrac{(R-1)L_f}{G_{ss}\tau}\right)\exp\left(-\dfrac{L}{G_{ss}\tau}\right) & \text{if } L \geq L_f. \end{cases} \tag{40}$$

Table 8
Errors and computational times of the method of characteristics applied to the semi-industrial crystallization case study ($t_{end} = 10800$ s and $dt = 10$ s).

	Case 1	Case 2	Case 3
Ngrids	2280	1200	270
CPU time (s)	167.6	58.3	34.0
m_0 error (%)	0.21	0.21	1.10
m_1 error (%)	0.14	0.14	0.65
m_2 error (%)	0.14	0.16	0.13
m_3 error (%)	0.21	0.27	0.38
m_4 error (%)	0.30	0.46	0.80
L_{mean} error (%)	0.09	0.20	0.42

In this equation, $R-1$ indicates the ratio between the product flow rate and the fines removal flow rate, whereas G_{ss} denotes the growth rate at the steady state. The model parameters are listed in Table 11.

Table 9
Errors and computational times of the various finite volume methods applied to the semi-industrial crystallization case study ($t_{end} = 10\,800$ s and $dt = 10$ s).

	First order	High order: van Leer	High order: Koren
CPU time (s)	24.6	24.8	24.9
m_0 error (%)	0.44	0.11	0.11
m_1 error (%)	0.86	0.33	0.31
m_2 error (%)	0.55	0.39	0.37
m_3 error (%)	1.84	0.29	0.26
m_4 error (%)	3.62	0.34	0.30
L_{mean} error (%)	1.75	0.05	0.04

Table 10
Errors and computational times of the various finite element methods applied to the semi-industrial crystallization case study ($t_{end} = 10800$ s and $dt = 10$ s).

	OCM: linear B.F. ($ne = 1200$)	OCM: Lagrange B.F. ($ne = 400,\ nc = 3$)	GFEM: Lagrange B.F. ($ne = 400,\ nc = 3$)
CPU time (s)	24.7	58.3	58.5
m_0 error (%)	4.13	1.66	1.65
m_1 error (%)	1.15	0.17	0.17
m_2 error (%)	1.01	0.16	0.17
m_3 error (%)	1.86	0.26	0.26
m_4 error (%)	3.39	0.39	0.38
L_{mean} error (%)	1.51	0.13	0.13

Table 11
Parameters of the continuous crystallization model.

Symbol	Parameter	Value	Unit
g	Growth rate exponent	0.676	–
k_b	Nucleation rate constant	5.95×10^9	#/m^3 s
k_g	Growth rate constant	1.5×10^{-6}	m/s
L_f	Crystal cut size	80.0×10^{-6}	m
$L_{0,g1}$	Location parameter of distribution	234.1×10^{-6}	m
L_{SN}	Integration bound in nucleation term	650.0×10^{-6}	m
Q_f	Fines flow rate	2.0×10^{-3}	m^3/s
Q_p	Product flow rate	2.5×10^{-4}	m^3/s
$\sigma_{g,1}$	Spread parameter of distribution	1.54	–
τ	Mean residence time in crystallizer	4400	s
τ_f	Mean residence time in fines removal section	645	s

The PBE model of this crystallization system is solved using the method of characteristics, the high order finite volume method with Koren flux limiting function and the finite element methods. Fig. 8 shows the natural logarithm of the predicted number density distribution at the steady state in comparison with the analytical solution. As can be seen, the method of characteristics and the high order finite volume method with the flux limiting function capture the sharp discontinuity fairly well, though the former numerical technique is much more computationally involved; see Table 12. This is due to the addition of a crystal cell at every time step that for a large process time of 129600 s amounts to a substantially great number of cells, making the application of the method of characteristics tremendously inefficient. In spite of the fact that the elimination of the redundant cells, while preserving the accuracy of the solution, restores the computational efficiency to a very large extent, the method of characteristics still has a much higher computational burden among the solution methods applied to this case study.

Fig. 8(c) and (d) yet again demonstrate that the finite element methods, namely the orthogonal collocation method and the Galerkin's technique using the Lagrange basis function, are incapable of dealing with the sharp discontinuities. Though the computational efficiency is comparable to that of the high order finite volume method with flux limiting function, the numerical predictions are much less accurate.

6. Conclusions

In this study, a number of numerical solution methods belonging to the family of the discretization techniques and the finite element methods have been used to simulate the dynamic behavior of various crystallization systems involving nucleation and growth processes. Numerical solution of the population balance equation pertaining to these systems is often complicated due to the occurrence of steep moving fronts and/or sharp discontinuities. These numerical difficulties normally arise from the convective nature of the partial differential equation and the incompatibility between its boundary and initial conditions for real crystallization systems.

Requirements on the numerical solution method greatly depend on the nature of the application as well as the crystallization system under consideration. The choice of the solution method should therefore be made in accordance with the settings of the problem at hand, implying that universal guidelines for the numerical method selection may be inadequate. Nonetheless, this paper provides an overview of the most widely used PBE solution methods that can be best used for on-line control applications.

From the test problems and the real crystallization case studies, it is found that the method of characteristics yields the most accurate numerical predictions as they are free from the diffusion problem due to elimination of the convection term in the population balance equation. The implementation of this method is however rather complicated since the spatial grid mesh, over which the crystal size distribution is discretized, is not fixed. Furthermore, a cell of nuclei should be added at regular time intervals to incorporate the nucleation term. Though the computational efficiency of the method of characteristics can be restored to a large extent by appropriate handling of the number of the moving crystal cells, there are still a number of limitations to its application, namely the determination of integration and cell addition time steps and the excessive computational burden when complex real systems are dealt with.

This study reveals that the high order finite volume methods with flux limiting functions are attractive alternatives to the method of characteristics. High order finite volume methods with flux limiting functions are well capable of capturing the sharp discontinuities and steep moving fronts, while they are much less prone to numerical diffusion in comparison with the first order upwind finite volume method. These schemes also benefit from ease of implementation and relatively low computational requirements as opposed to other solution methods considered in this work. The latter feature of the high order finite volume methods with flux limiting functions allows one to utilize a finer grid mesh to further enhance the numerical accuracy of the method at the cost of reasonable computational effort.

Contrary to the above discussed solution methods, the finite element methods appear to be less appealing. Though the orthogonal collocation method with the linear basis function yields improved stability, the predictions often suffer from severe numerical diffusion that is comparable to the first order finite volume method. It is observed that the orthogonal collocation and Galerkin's finite element methods using the Lagrange basis function may lead to more accurate predictions; often at the cost of much higher computational effort. This is due to the fact that the higher order basis functions require far more computations and interpolations than the linear basis functions. In addition to the complex implementation of the finite element methods using the Lagrange basis function, their applicability is largely dependent on the problem under investigation. These methods typically result in severe oscillations that cannot be alleviated neither by introducing an artificial diffusion term nor by increasing the number of elements.

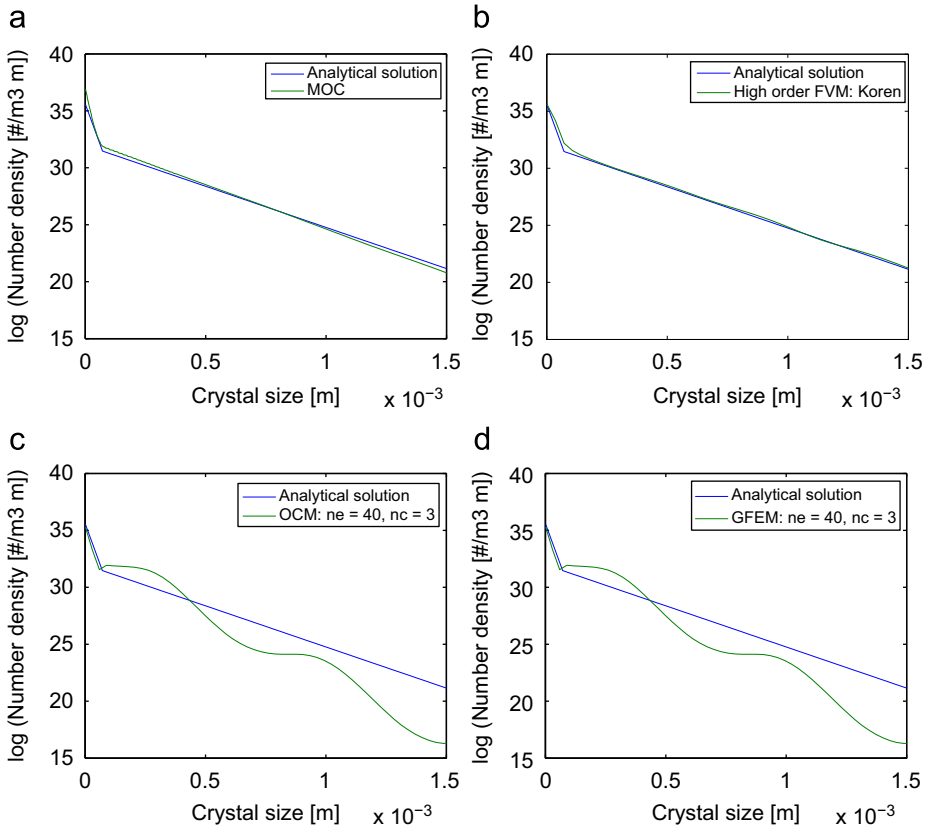

Fig. 8. Natural logarithm of the crystal size distribution obtained at the steady state of the continuous crystallizer. (a) Method of characteristics. (b) High order FVM: Koren. (c) Orthogonal collocation (Lagrange basis function). (d) Galerkin on finite element (Lagrange basis function).

Table 12
Errors and computational times of the solution methods applied to the continuous crystallization case study ($t_{end} = 129\,600$ s and $dt = 10$ s).

	Ngrids	CPU time (s)	m_0 error (%)	m_3 error (%)
MOC	229	3501.12	0.07	0.24
High order FVM: Koren	100	700.65	0.17	0.38
OCM: lagrange B.F.	120	769.32	1.27	2.74
GFEM: Lagrange B.F.	120	787.11	1.26	2.73

Acknowledgments

The work presented in this paper was carried out within the EUREKA/IS-project E! 3458/IS043074, called CryPTO (Crystallizer based Processing: fundamenTal research into mOdelling). The financial support of SenterNovem is gratefully acknowledged.

References

Alexopoulos, A.H., Kiparissides, C., 2005. Part II: dynamic evolution of the particle size distribution in particulate processes undergoing simultaneous particle nucleation, growth and aggregation. Chemical Engineering Science 60, 4157–4169.

Alexopoulos, A.H., Roussos, A.I., Kiparissides, C., 2004. Part I: dynamic evolution of the particle size distribution in particulate processes undergoing combined particle growth and aggregation. Chemical Engineering Science 59, 5751–5769.

Baterham, R.J., Hall, J.S., Barton, G., 1981. Pelletizing kinetics and simulation of full scale balling circuits. In: Proceedings of the Third International Symposium on Agglomeration, Nurnberg, West Germany, pp. A136–A144.

Bennett, M.K., Rohani, S., 2001. Solution of population balance equations with a new combined Lax–Wendroff/Crank–Nicholson method. Chemical Engineering Science 56, 6623–6633.

Chen, M.Q., Hwang, C., Shih, Y.P., 1996. A wavelet-Galerkin method for solving population balance equations. Computers & Chemical Engineering 20, 131–145.

Costa, C.B.B., Maciel, M.R.W., Filho, R.M., 2007. Considerations on the crystallization modeling: population balance equation. Computers & Chemical Engineering 31, 206–218.

Crowley, T.J., Meadows, E.S., Kostoulas, E., Doyle III, F.J., 2000. Control of particle size distribution described by a population balance model of semi-batch emulsion polymerization. Journal of Process Control 10, 419–432.

David, R., Villermaux, J., Marchal, P., Klein, J.P., 1991. Crystallization and precipitation engineering—IV. Kinetic model of adipic acid crystallization. Chemical Engineering Science 46, 1129–1136.

David, R., Paulaime, A.M., Espitalier, F., Rouleau, L., 2003. Modeling of multiple-mechanism agglomeration in a crystallization process. Powder Technology 130, 338–344.

Eyre, D., Wright, C.J., Reuter, G., 1988. Spline-collocation with adaptive mesh grading for solving the stochastic collection equation. Journal of Computational Physics 78, 288–304.

Ferziger, J.H., Peric, M., 1996. Computational Methods for Fluid Dynamics. Springer, Berlin.

Finlayson, B.A., 1980. Nonlinear Analysis in Chemical Engineering. McGraw-Hill, New York.

Gelbard, F., Seinfeld, J.H., 1978. Numerical solution of the dynamical equation for particulate systems. Journal of Computational Physics 28, 357–375.

Gerstlauer, A., Mitrovic, A., Motz, S., Gilles, E.D., 2001. A population model for crystallization processes using two independent particle properties. Chemical Engineering Science 56, 2553–2565.

Gunawan, R., Fusman, I., Braatz, R.D., 2004. High resolution algorithms for multidimensional population balance equations. A.I.Ch.E. Journal 50, 2738–2749.

Hounslow, M.J., Ryall, R.L., Marshall, V.R., 1988. A discretized population balance for nucleation, growth and aggregation. A.I.Ch.E. Journal 34 (11), 1821–1832.

Hu, Q., Rohani, S., Jutan, A., 2005a. Modelling and optimization of seeded batch crystallizers. Computers & Chemical Engineering 29, 911–918.

Hu, Q., Rohani, S., Jutan, A., 2005b. New numerical method for solving the dynamic population balance equations. A.I.Ch.E. Journal 51 (11), 3000–3006.

Hulbert, H.M., Katz, S., 1964. Some problems in particle technology: a statistical mechanical formulation. Chemical Engineering Science 9, 555–574.

Koren, B., 1993. A robust upwind discretization method for advection, diffusion and source terms. In: Vreugdenhill, C.B., Koren, B. (Eds.), Numerical Methods for Advection–diffusion Problems, vol. 22, pp. 117–138.

Kumar, S., Ramkrishna, D., 1997. On the solution of population balance equations by discretization—III. Nucleation, growth and aggregation of particles. Chemical Engineering Science 52, 4659–4679.

Lapidus, L., Pinder, G.F., 1982. Numerical Solution of Partial Differential Equations in Science and Engineering. Wiley, New York.
LeVeque, R.J., 2002. Finite Volume Methods for Hyperbolic Problems. Cambridge University Press, New York.
Lim, Y.L.L., Lann, J.M.L., Meyer, X.M., Joulia, X., Lee, G., Yoon, E.S., 2002. On the solution of population balance equations (PBE) with accurate front tracking methods in practical crystallization processes. Chemical Engineering Science 57, 3715–3732.
Litster, J.D., Smit, D.J., Hounslow, M.J., 1995. Adjustable discretized population balance for growth and aggregation. A.I.Ch.E. Journal 41, 591–603.
Liu, Y., Cameron, I.T., 2003. A new wavelet-based adaptive method for solving population balance equations. Powder Technology 130, 181–188.
Ma, A., Tafti, D.K., Braatz, R.D., 2002. High resolution simulation of multidimensional crystal growth. Industrial & Engineering Chemistry Research 41, 6217–6223.
Mahoney, A., Ramkrishna, D., 2002. Efficient solution of population balance equations with discontinuities by finite elements. Chemical Engineering Science 57, 1107–1119.
Maisels, A., Kruis, F.E., Fissan, H., 1999. Direct Monte Carlo simulations of coagulation and aggregation. Journal of Aerosol Science 30, S417–S418.
Marchal, P., David, R., Klein, J.P., Villermaux, J., 1990. Crystallization and precipitation engineering—I. An efficient method for solving population balances in crystallization with agglomeration. Chemical Engineering Science 43, 59–67.
Matthews, H.B., Rawlings, J.B., 1998. Batch crystallization of a photochemical: modeling, control and filtration. A.I.Ch.E. Journal 44, 1119–1127.
Meimaroglou, D., Roussos, A.I., Kiparissides, C., 2006. Part IV: dynamic evolution of the particle size distribution in particulate processes. A comparative study between Monte Carlo and the generalized method of moments. Chemical Engineering Science 61, 5620–5635.
Mesbah, A., Kalbasenka, A.N., Huesman, A.E.M., Kramer, H.J.M., Van den Hof, P.M.J., 2008. Real-time dynamic optimization of batch crystallization processes. In: Proceedings of the 17th IFAC World Congress, Seoul, Korea, pp. 3246–3251.
Motz, S., Mitrovic, A., Gilles, E.D., Vollmer, U., Raisch, J., 2003. Modeling, simulation and stabilizing H_∞-control of an oscillating continuous crystallizer with fines dissolution. Chemical Engineering Science 58, 3473–3488.
Muhr, H., David, R., Villermaux, J., Jezequel, P.H., 1996. Crystallization and precipitation engineering—VI. Solving population balance in the case of the precipitation of silver bromide crystals with high primary nucleation rates by using the first order upwind differentiation. Chemical Engineering Science 51, 309–319.
Nagy, Z.K., 2009. Model based robust control approach for batch crystallization product design. Computers & Chemical Engineering, in press, doi:10.1016/j.compchemeng.2009.04.012.
Nicmanis, M., Hounslow, M.J., 1998. Finite element methods for steady-state population balance equations. A.I.Ch.E. Journal 44, 2258–2272.
Ottens, E.P.K., Janse, A.H., de Jong, E.J., 1972. Secondary nucleation in a stirred vessel cooling crystallizer. Journal of Crystal Growth 13/14, 500–505.
Paengjuntuek, W., Arpornwichanop, A., Kittisupakorn, P., 2008. Product quality improvement of batch crystallizers by a batch-to-batch optimization and nonlinear control approach. Chemical Engineering Journal 139, 344–350.
Patankar, S., 1980. Numerical Heat Transfer and Fluid Flow. Hemisphere Publishing, New York.
Qamar, S., Warnecke, G., 2007. Numerical solution of population balance equations for nucleation, growth and aggregation processes. Computers & Chemical Engineering 31, 1576–1589.
Qamar, S., Elsner, M.P., Angelov, I.A., Warnecke, G., Seidel-Morgenstern, A., 2006. A comparative study of high resolution schemes for solving population balances in crystallization. Computers & Chemical Engineering 30, 1119–1131.
Ramkrishna, D., 2000. Population Balances: Theory and Applications to Particulate Systems in Engineering. Academic Press, San Diego.
Ramkrishna, D., 1985. The status of population balances. Reviews in Chemical Engineering 3 (1), 49–95.
Randolph, A.D., Larson, M.A., 1988. Theory of Particulate Processes. second ed. Academic Press, San Diego.
Rawlings, J.B., Miller, S.M., Witkowski, W.R., 1993. Model identification and control of solution crystallization processes: a review. Industrial & Engineering Chemistry Research 32, 1275–1296.
Rigopoulos, S., Jones, A.G., 2003. Finite-element scheme for solution of the dynamic population balance equation. A.I.Ch.E. Journal 49, 1127–1139.
Roussos, A.I., Alexopoulos, A.H., Kiparissides, C., 2005. Part III: dynamic evolution of the particle size distribution in batch and continuous particulate processes: a Galerkin on finite elements approach. Chemical Engineering Science 60, 6998–7010.
Sandu, A., Borden, C., 2003. A framework for the numerical treatment of aerosol dynamics. Applied Numerical Mathematics 45, 475–497.
Shi, D., El-Farra, N.H., Mhaskar, P., Li, M., Christofides, P.D., 2006. Predictive control of particle size distribution in particulate processes. Chemical Engineering Science 61, 268–281.
Song, M., Qiu, X.J., 1999. Alternative to the concept of the interval of quiescence (IQ) in the Monte Carlo simulation of population balances. Chemical Engineering Science 54, 5711–5715.
van Leer, B., 1985. Upwind-difference methods for aerodynamic problems governed by the Euler equations. In: Lectures in Applied Mathematics, vol. 22. American Mathematical Society, pp. 327–336.
Versteeg, H.K., Malalasekera, W., 1995. An Introduction to Computational Fluid Dynamics. The Finite Volume Method. Longman Group, Malaysia.
Wojcik, J.A., Jones, A.G., 1998. Dynamics and stability of continuous MSMPR agglomerative precipitation: numerical analysis of the dual particle co-ordinate model. Computers & Chemical Engineering 22, 535–545.
Wulkow, M., Gerstlauer, A., Nieken, U., 2001. Modeling and simulation of crystallization processes using PARSIVAL. Chemical Engineering Science 56, 2575–2588.